Fukuyama and Suzuki *Earth, Planets and Space* (2016) 68:194
DOI 10.1186/s40623-016-0570-6

Earth, Planets and Space

LETTER

Open Access

Near-fault deformation and Dc″ during the 2016 Mw7.1 Kumamoto earthquake

Eiichi Fukuyama* and Wataru Suzuki

Abstract

An Mw7.1 Kumamoto earthquake occurred at 01:25:05 on April 16, 2016 (JST). The earthquake involved a rupture at a shallow depth along a strike-slip fault with surface breaks. Near-fault ground motion records, especially those of a strike-slip earthquake, can provide us with direct information on the earthquake source process. During the earthquake, near-fault seismograms were obtained at KMMH16 station located about 500 m off the fault. The ground displacements were well recovered from the double numerical integration of accelerograms at KMMH16 both on the surface and at the bottom of the 252-m-deep borehole. Fault-parallel static displacement was estimated to be about 1.1 m from the acceleration waveforms. The Dc″ value, which is defined as double the fault-parallel displacement at peak velocity time, was proposed as a proxy of the slip-weakening distance. Using both the velocity and displacement fault-parallel waveforms, the Dc″ value was estimated at about 1 m. This value was between 30 and 50% of the total slip on the fault, which is consistent with previous observations.

Keywords: Near-fault displacement, Slip-weakening distance, Strike-slip fault

Introduction

Ida (1972) proposed a slip-weakening friction law for shear faulting, where friction decreases gradually from the peak friction level to the residual level. In the slip-weakening law, slip-weakening distance (Dc) is defined as the slip needed to reach the residual friction. Dc is considered to be one of the important parameters for characterizing the unstable rupture propagation (e.g., Ohnaka 2013), since slip-weakening behavior represents an important feature of earthquake dynamic rupture propagation.

Ide and Takeo (1997) proposed a method to estimate a slip-weakening distance using the spatiotemporal slip history on the fault; they estimated it as 0.5–1 m for the 1995 Kobe earthquake. In their method, a complete description of the spatiotemporal distribution of the slip on the fault is required, which is usually difficult to estimate reliably. Twardzik et al. (2014) tried to invert observed waveforms of the 2004 Parkfield earthquake to directly obtain the dynamic parameters including the slip-weakening distance. However, as Guatteri and Spudich (2000) suggested, fracture energy could be estimated more stably than Dc when the data do not include sufficient high-frequency waves. Goto and Sawada (2010) discussed the trade-offs among the dynamic parameters when inverting the observed waveforms. Tinti et al. (2005) estimated the fracture energy distribution on the fault using a kinematic slip model. Fracture energy can be stably estimated by integrating the shear stress up to the slip-weakening distance. Therefore, a simple method for the estimation of slip-weakening distance is required.

Mikumo et al. (2003) proposed Dc′ as a proxy of Dc. Usually, to estimate a Dc value, both stress and slip functions are needed at a point on the fault. To estimate the stress function, the whole spatiotemporal history of the slip function on the fault is required, as has been done by Ide and Takeo (1997). However, Dc′ can be estimated using only the slip and slip velocity functions at a point on the fault, and the stress function is not needed. Dc″ proposed by Fukuyama and Mikumo (2007) is an approximated quantity of Dc′ used to roughly estimate the Dc value from the near-fault seismograms; Dc″ is an off-fault version of Dc′.

*Correspondence: fuku@bosai.go.jp
National Research Institute for Earth Science and Disaster Resilience, Tsukuba 305-0006, Japan

Recently, the Kumamoto earthquake sequence started at 21:26:34 on April 14, 2016 (JST, UT+9h), with an Mw6.1 earthquake that occurred on the Hinagu fault. Twenty-eight hours later, an Mw7.1 earthquake initiated at 01:25:05 on April 16, 2016 (JST), in nearly the same location and it ruptured eastward along the Futagawa fault as well as the Hinagu fault (Fig. 1). Its hypocenter was located at Lat. 32.7539°N, Long. 130.7648°E and at a depth 13.1 km by Hi-net (NIED 2016a). From the moment tensor analysis, the focal mechanism was determined to be a strike-slip type with a tension axis oriented north–south (NIED 2016b). The rupture propagated almost unilaterally toward the northeast for about 30 km (e.g., Kubo et al. 2016).

It should be noted that between these Mw6.1 and Mw7.1 earthquakes, Mw 5.4 (22:07:35 on April 14, 2016, JST) and Mw 6.0 (00:03:46 on April 15, 2016, JST) earthquakes occurred inside the aftershock area of the Mw 6.1 earthquake (NIED 2016c). This suggests that an unusual level of aftershock activity for the Mw 6.1 earthquake, in view of their locations and magnitudes, preceded the Mw 7.1 earthquake (e.g., Kato et al. 2016).

Since the National Research Institute for Earth Science and Disaster Resilience (NIED) has nationwide strong motion seismic networks called K-NET (Kinoshita 1998) and KiK-net (Okada et al. 2004; Aoi et al. 2011), several near-fault seismograms were recorded during this earthquake. Among these waveforms, the waveforms at KMMH16 (Lat. 32.7967°N, Long. 130.8199°E, height 55 m, see Fig. 1) were exceptional, in the sense that they were obtained close to the fault both on the surface and at the bottom of a 252-m-deep borehole. From our limited knowledge, this observation could be the first in which both surface and borehole seismograms were obtained close to the strike-slip faulting, although Fukuyama (2015) reported the near-fault surface and borehole seismograms that were recorded during the reverse faulting of the 2008 Iwate–Miyagi Nairiku earthquake (Mw 6.9).

The near-fault seismograms of vertical strike-slip earthquakes are very important for directly measuring the earthquake source properties. It is well known that because of very little excitation of Rayleigh waves (Okada

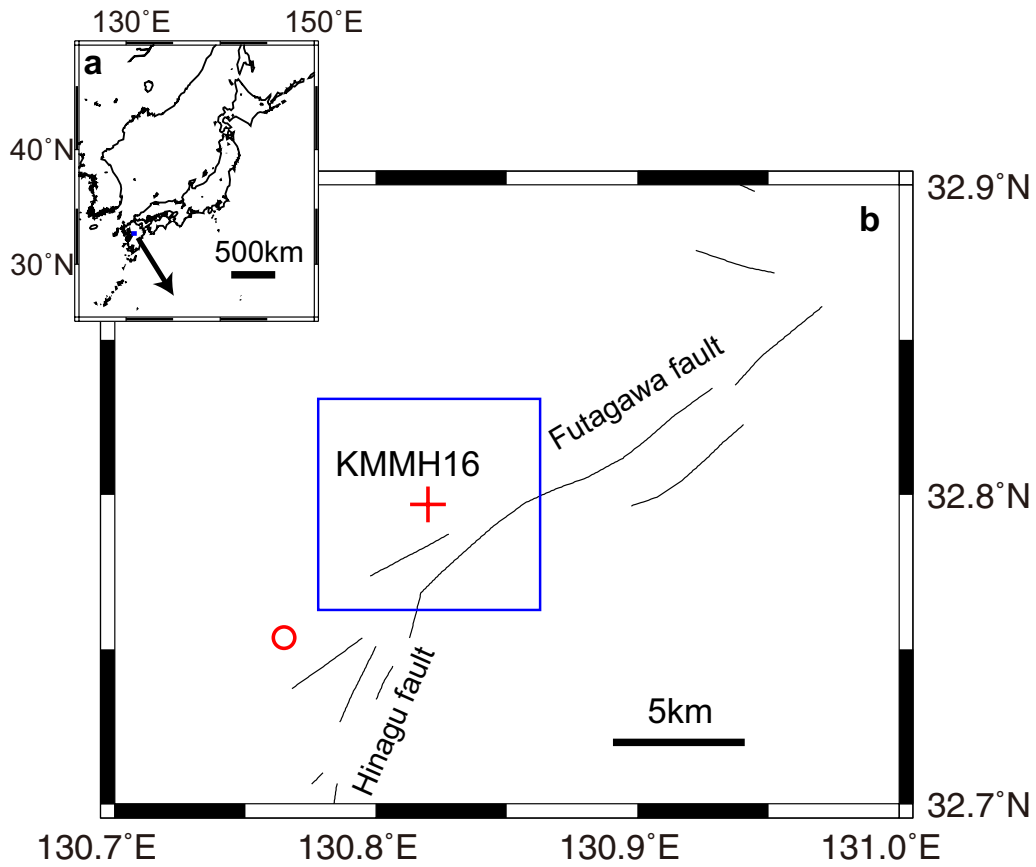

Fig. 1 Location of the station and active fault traces. *Blue solid rectangle* in **a** indicates the area shown in **b**. *Solid lines* in **b** indicate the active fault trace. *Red cross* in **b** shows the location of KMMH16 station. *Red open circle* indicates the epicenter location of the Mw7.1 Kumamoto earthquake. *Blue open rectangle* in **b** indicates the area shown in Fig. 2

1992; Zhang and Chen 2006), the free surface effect becomes negligible and the "Method of Images" can be applied to compute the fault slip history in full space. Then, the observed near-fault seismogram for a vertical strike-slip event can be considered as if it is observed at the middle of the fault at depth.

Once we directly measure the fault-parallel ground motion close to the fault, we will be able to estimate the slip-weakening distance from that observation as Dc″ as proposed by Fukuyama and Mikumo (2007). Dc″ is estimated using the near-fault seismograms that are obtained close to the vertical strike-slip fault. Dc″ is defined as double the fault-parallel ground displacement when the absolute fault-parallel ground velocity is at a maximum (Fukuyama and Mikumo 2007). Cruz-Atienza et al. (2009) investigated the accuracy of the Dc″ estimation using numerical simulations. They concluded that the estimation of Dc″ could be reasonable if the station is located within the distance of Rc (the resolution distance), which is approximately 0.8 times the wavelength at breakdown frequency.

In this manuscript, we investigate the near-fault ground deformation using a set of seismograms observed close to the fault at KMMH16 station. In addition, since this Mw 7.1 earthquake had vertical strike-slip faulting, the ground displacement very close to the fault can be considered a proxy of the fault slip motion. Using this near-fault displacement at KMMH16, we estimate the Dc″ value for the 2016 Mw7.1 Kumamoto earthquake.

Methods

We used the waveforms recorded at the KiK-net station KMMH16. This station is located about 500 m away from the fault trace, which can be identified by InSAR measurements (Fig. 2). The InSAR image (GSI 2016; Fujiwara et al. 2016) was based on the residual between the February 10, 2015, and April 19, 2016, measurements, which included both the deformations of the Mw 6.1 and Mw 7.1 earthquakes. However, it was reported that the ground deformation near the KMMH16 station was small due to the Mw 6.1 earthquake based on the InSAR analysis between November 14, 2014, and 12:52 (JST) of April 15, 2016 (e.g., Ozawa et al. 2016). We identified the fault trace using the InSAR image of Fig. 2b, c. We assumed that the fault trace should be rather straight, so we took the northern boundary that appears in the InSAR image, also taking into account the hypocenter location. Then, we measured the distance from the fault to station KMMH16.

To obtain the displacement waveforms, we first subtracted a constant value from each original acceleration waveform to set the onset acceleration to zero. Then, we numerically integrated the original acceleration waveforms twice in the time domain. We rotated the seismograms to fault-parallel (N235°E) and fault-normal (N325°E) directions. We corrected the instrument response by multiplying the waveforms by a constant value to convert the recorded digits to the physical value of acceleration. It should be noted that we did not apply any low-pass or high-pass filtering operations. Therefore, we did not correct the frequency response of the sensor. However, since our focus here is the near-fault displacement and acceleration response at low frequency is flat, the uncorrected high-frequency response does not affect the present analysis.

The obtained seismograms are shown in Fig. 3. It should be noted that the ground displacements are quite similar both on the surface and at the bottom of the borehole. Since the fault motion dominated the right-lateral strike slip, no tilt component along the fault surface was expected. Therefore, the agreement of the displacement between that on the surface and that at the borehole is quite consistent with the theoretical prediction. Strike-slip fault motion did not cause significant ground rotation whose axis was directed parallel to the fault strike (e.g., Okada 1992).

Results and discussion

In Fig. 3, acceleration, velocity and displacement seismograms are shown. As can be seen, the maximum amplitudes of the accelerations were quite different between the acceleration on the surface and that at the bottom of the borehole. However, the velocity and displacement behaved similarly in these two locations. Since the fault slip motion dominates the right-lateral strike slip, the displacements recorded by these two sensors should be quite similar to those expected theoretically as stated above.

Near the KMMH16 station, Kumamoto prefecture installed an accelerometer at Mashiki town hall (Miyazono, Fig. 2a). Iwata (2016) numerically integrated the accelerogram to obtain the displacement. We confirmed that the fault-parallel and fault-normal displacements at Miyazono were almost identical to those at KMMH16. In addition, the vertical displacement at Miyazono was identical to the vertical displacement at the surface of KMMH16. These similarities warrant the accuracy of ground displacements measured by accelerometers. A small difference between the vertical displacements on the surface and at the bottom of the borehole at KMMH16 might be significant. The amount of strain change can be roughly estimated as 8×10^{-4}, which is much larger than the value ($\sim 10^{-6}$) expected from the slip model of the Mw7.1 earthquake (e.g., Ozawa et al. 2016). In this study, we are not going into further detail regarding this difference.

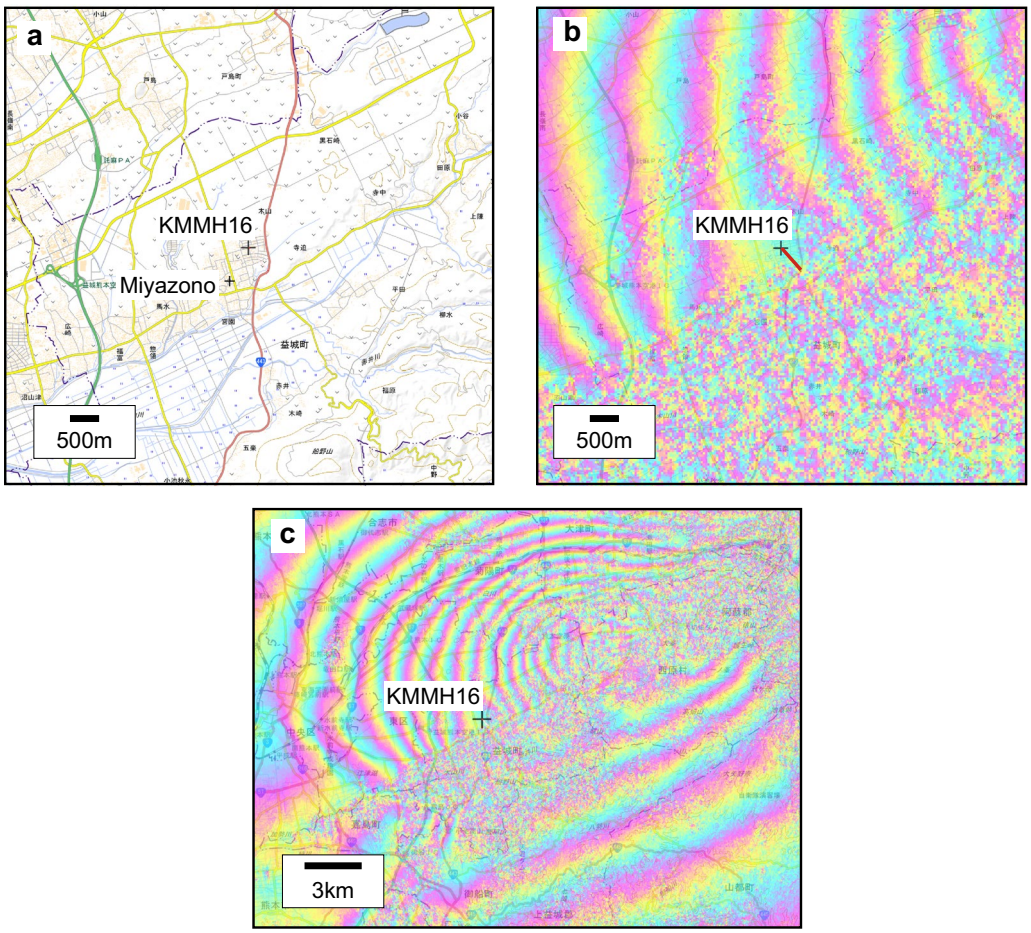

Fig. 2 **a** Local map near the station KMMH16 (*black plus*). **b** InSAR image overlaid with the local map of **a**. *Black plus* is the same as **a**. *Red straight line* shows the shortest length to the fault trace. **c** InSAR image for the area of Fig. 1b. These maps are taken from GSI (2016). Regarding the InSAR data, analysis was done by GSI using ALOS-2 raw data of JAXA which was provided through the SAR Analysis Working Group of the Coordinating Committee for the Earthquake Prediction

In Fig. 4, we show a comparison between the velocity and displacement waveforms. Following Fukuyama and Mikumo (2007), the value of Dc″ can be estimated by measuring the amount of displacement when the ground velocity reaches a peak (maximum or minimum) and multiplying by two to convert the ground displacement to the fault slip. The Dc″ values are estimated to be 1 m (Fig. 4). However, one should be careful when using Dc″ as an approximation of Dc. According to Mikumo et al. (2003) and Fukuyama and Mikumo (2007), Dc″ includes about a 50% error when estimating Dc.

The Dc″ value for the Kumamoto earthquake is between the 2000 Mw6.6 Western Tottori earthquake at GSH station (Dc″ = 0.3 m) and the 2002 Mw7.9 Denali earthquake at PS10 station (Dc″ = 2.5 m) (Fig. 5). The two prediction lines in Fig. 5 were taken from Mikumo et al. (2003), and these stand for the possible range of the relation between the slip-weakening distance and the total slip distance. These observations suggest that the slip-weakening distance is a fraction of the total amount of slip, i.e., Dc″ is about 30–50% of the measured total slip. This feature is also consistent with the observation by Abercrombie and Rice (2005) that the fracture energy is scale dependent.

If more Dc″ data are collected in the future, our understanding of the slip-weakening distance during earthquakes will significantly improve. This is important because during the unstable rupture of earthquakes, the slip-weakening distance plays an important role in the propagation of the rupture.

As stated before, Cruz-Atienza et al. (2009) proposed Rc (the resolution distance) to evaluate the accuracy

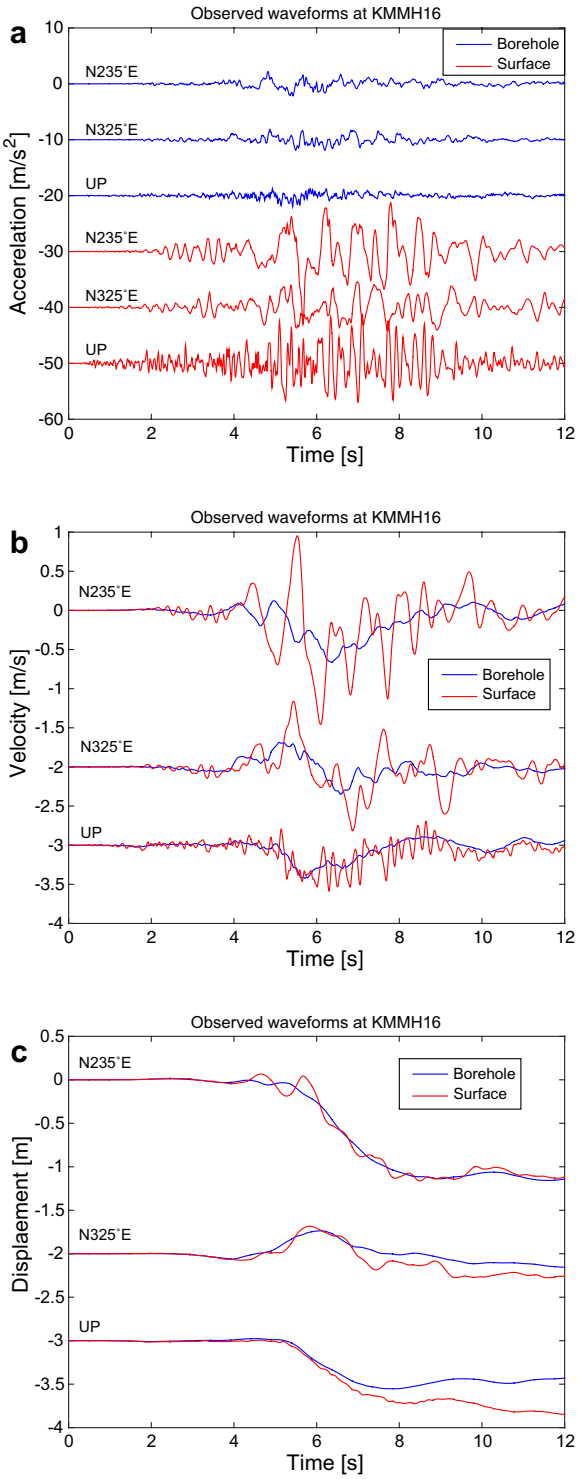

Fig. 3 Observed waveforms at KMMH16 station. Horizontal components were rotated to fault-parallel (N235°E) and fault-normal (N325°E) directions. **a** Acceleration seismograms observed at the *bottom* of borehole (*blue*) and on the surface (*red*), **b** velocity seismograms and **c** displacement seismograms. Origin in time axis is taken at the first arrival of the signal (01:25:08 on April 16, 2016, JST)

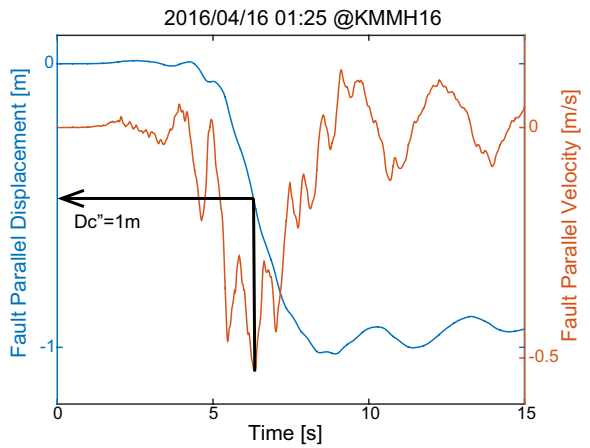

Fig. 4 Fault-parallel velocity and displacement at KMMH16 are plotted for the estimation of the Dc″ value

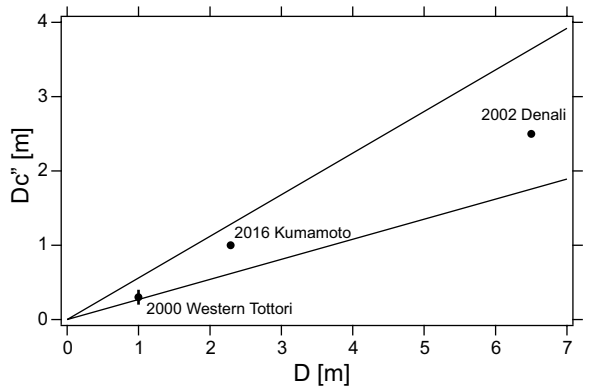

Fig. 5 Comparison between the final slip D and estimated Dc″ values for the 2000 Western Tottori earthquake estimated at GSH station, the 2002 Denali at PS10 station and the 2016 Kumamoto at KMMH16 station. *Two solid lines* stand for the upper and lower limits of Dc (Dc″ = 0.56 D and Dc″ = 0.27 D, respectively) estimated by Mikumo et al. (2003). Modified from Fig. 4 of Fukuyama and Mikumo (2007)

of Dc″. They proposed that Rc = 0.8 Vs Tc where Vs is the shear wave velocity and Tc is the breakdown time. Vs is 2.7 km/s taken from the logging profile of this station (NIED 2016d). Tc was estimated at about 1.1 s from the time when the displacement started to accelerate until the peak ground velocity occurred (Fig. 4). Thus, in the present case, Rc becomes about 2.4 km. The distance from KMMH16 to the fault is much smaller than this estimate (Fig. 2). Therefore, the present observations were done inside the Rc, and we consider that the estimated value has some meaning on the slip-weakening distance. At the very least, the present estimation suggests the upper bound of the slip-weakening distance.

Conclusions

We investigated the near-fault displacement field using the accelerograms obtained at KMMH16, a KiK-net station, where waveforms were recorded both on the surface and at the bottom of a 252-m-deep borehole. The displacement behavior was similar at both locations, which is consistent with strike-slip fault motion. By using the fault-parallel velocity and displacement, we estimated a Dc″ of 1 m, which could be considered at least as the upper bound value of the slip-weakening distance on the fault. This Dc″ value is consistent with previous estimates, and it falls between 30 and 50% of the measured total slip at the near-fault station.

Authors' contributions

EF analyzed the data and wrote the manuscript, while WS collected the observed waveforms and the related information. Both authors read and approved the final manuscript.

Acknowledgements

Waveform data were provided by the KiK-net maintained by the National Research Institute for Earth Science and Disaster Resilience. Comments by two anonymous reviewers were quite valuable.

Competing interests

The authors declare that they have no competing interests.

Received: 29 June 2016 Accepted: 17 November 2016
Published online: 29 November 2016

References

Abercrombie RE, Rice JR (2005) Can observation of earthquake scaling constrain slip weakening? Geophys J Int 162:406–424. doi:10.1111/j.1365-246X.2005.02579.x

Aoi S, Kunugi T, Nakamura H, Fujiwara H (2011) Deployment of new strong motion seismographs of K-NET and KiK-net. In: Akkar S, Gulkan P, van Eck T (eds) Earthquake data in engineering seismology. Springer, Netherlands, pp 167–186

Cruz-Atienza VM, Olsen KB, Dalguer LA (2009) Estimation of the breakdown slip from strong-motion seismograms: insights from numerical experiments. Bull Seismol Soc Am 99(6):3454–3469. doi:10.1785/0120080330

Fujiwara S, Yarai H, Kobayashi T, Morishita Y, Nakano T, Miyahara B, Nakai H, Miura Y, Ueshiba H, Kakiage Y, Une H (2016) Small-displacement linear surface ruptures of the 2016 Kumamoto earthquake sequence detected by ALOS-2 SAR interferometry. Earth Planets Space 68:160. doi:10.1186/s40623-016-0534-x

Fukuyama E (2015) Dynamic faulting on a conjugate fault system detected by near-fault tilt measurements. Earth Planets Space 67:38. doi:10.1186/s40623-015-0207-1

Fukuyama E, Mikumo T (2007) Slip-weakening distance estimated at near-fault stations. Geophys Res Lett 34:L09302. doi:10.1029/2006GL029203

Goto H, Sawada S (2010) Trade-offs among dynamic parameters inferred from results of dynamic source inversion. Bull Seismol Soc Am 100(3):910–922. doi:10.1785/0120080250

GSI (2016) http://www.gsi.go.jp/BOUSAI/H27-kumamoto-earthquake-index.html, http://maps.gsi.go.jp/#10/32.942420/130.719452/&base=std&ls=std%7Curgent_earthquake_20160414kumamoto_20150209_20160418_v03r%2C0.7%7Ctoshiken_katsudansouzu%7C20160414kumamoto_epicenter&disp=1111&lcd=20160414kumamoto_epicenter&vs=c1j0l0u0f0&d=v. Accessed 22 June 2016

Guatteri M, Spudich M (2000) What can strong motion data tell us about slip-weakening fault friction laws? Bull Seismol Soc Am 90(1):98–116. doi:10.1785/0119990053

Ida Y (1972) Cohesive force across the tip of a longitudinal-shear crack and Griffith's specific surface energy. J Geophys Res 77(20):3796–3805. doi:10.1029/JB077i020p03796

Ide S, Takeo M (1997) Determination of constitutive relations of fault slip based on seismic wave analysis. J Geophys Res 102(B12):27379–27391. doi:10.1029/97JB02675

Iwata T (2016) http://sms.dpri.kyoto-u.ac.jp/topics/masiki-nishihara0428ver2.pdf. Accessed 21 June 2016

Kato A, Fukuda J, Nakagawa S, Obara K (2016) Foreshock migration preceding the 2016 Mw 7.0 Kumamoto earthquake, Japan. Geophy Res Lett. doi:10.1002/2016GL070079

Kinoshita S (1998) Kyoshin net (K-NET). Seismol Res Lett 69(4):309–332. doi:10.1785/gssrl.69.4.309

Kubo H, Suzuki W, Aoi S, Sekiguchi H (2016) Source rupture processes of the 2016 Kumamoto, Japan, earthquakes estimated from strong motion waveforms. Earth Planets Space 68:161. doi:10.1186/s40623-016-0536-8

Mikumo T, Olsen KB, Fukuyama E, Yagi Y (2003) Stress-breakdown time and slip-weakening distance inferred from slip-velocity function on earthquake faults. Bull Seismol Soc Am 93(1):264–282. doi:10.1785/0120020082

NIED (2016a) http://www.hinet.bosai.go.jp/hypo/hinet/largeEQ/20160416000099:10.jma.png. Accesses 24 Oct 2016

NIED (2016b) http://www.fnet.bosai.go.jp/event/tdmt.php?_id=20160415162400&LANG=en. Accessed 24 Oct 2016

NIED (2016c) http://www.hinet.bosai.go.jp/topics/nw-kumamoto160416/?LANG=en. Accessed 24 Oct 2016

NIED (2016d) http://www.kyoshin.bosai.go.jp/cgi-bin/kyoshin/db/siteimage.cgi?1+KMMH16+kik+def. Accessed 24 Oct 2016

Ohnaka M (2013) The physics of rock failure and earthquakes. Cambridge University Press, Cambridge

Okada Y (1992) Internal deformation due to shear and tensile faults in a half-space. Bull Seismol Soc Am 82(2):1018–1040

Okada Y, Kasahara K, Hori S, Obara K, Sekiguchi S, Fujiwara H, Yamamoto A (2004) Recent progress of seismic observation networks in Japan—Hi-net, F-net, K-NET and KiK-net. Earth Planets Space 56:xv–xxviii. doi:10.1186/BF03353076

Ozawa T, Fujita E, Ueda H (2016) Crustal deformation associated with the 2016 Kumamoto earthquake and its effect on the magma system of Aso volcano. Earth Planets Space 68:186. doi:10.1186/s40623-016-0563-5

Tinti E, Spudich P, Cocco M (2005) Earthquake fracture energy inferred from kinematic rupture models on extended faults. J Geophys Res 110:B12303. doi:10.1029/2005JB003644

Twardzik C, Das S, Madariaga R (2014) Inversion for the physical parameters that control the source dynamics of the 2004 Parkfield earthquake. J Geophys Res Solid Earth 119:7010–7027. doi:10.1002/2014JB011238

Zhang HM, Chen XF (2006) Dynamic rupture on a planar fault in three-dimensional half space—I. Theory. Geophys J Int 164:633–652. doi:10.1111/j.1365-246X.2006.02887.x